Open access • Journal Article • DOI:10.1029/2009JD012786

Detection of volcanic SO2, ash, and H2SO4 using the Infrared Atmospheric Sounding Interferometer (IASI) — Source link

Federico Karagulian, Lieven Clarisse, Cathy Clerbaux, Cathy Clerbaux ...+3 more authors

Institutions: Université libre de Bruxelles, University of Paris, Norwegian Institute for Air Research

Published on: 27 Jan 2010 - Journal of Geophysical Research (John Wiley & Sons, Ltd)

Topics: Infrared atmospheric sounding interferometer, Atmospheric radiative transfer codes, Radiance, Volcano and Extinction (optical mineralogy)

Detection of volcanic SO2, ash and H2SO4 using the Infrared Atmospheric Sounding Interferometer (IASI)

F. Karagulian, Lieven Clarisse, Cathy Clerbaux, A. J. Prata, Daniel Hurtmans, Pierre-François Coheur

JOURNAL OF GEOPHYSICAL RESEARCH, VOL. 115, D00L02, doi:10.1029/2009JD012786, 2010

Detection of volcanic SO_2, ash, and H_2SO_4 using the Infrared Atmospheric Sounding Interferometer (IASI)

F. Karagulian,[1] L. Clarisse,[1] C. Clerbaux,[1,2] A. J. Prata,[3] D. Hurtmans,[1] and P. F. Coheur[1]

Received 6 July 2009; revised 24 September 2009; accepted 2 October 2009; published 27 February 2010.

[1] In this work we use infrared spectra recorded by the Infrared Atmospheric Sounding Interferometer (IASI) to characterize the emissions from the Mount Kasatochi volcanic eruption on 7 and 8 August 2008. We first derive the total atmospheric load of sulfur dioxide (SO_2) and its evolution over time. For the initial plume, we found values over 1.7 Tg of SO_2, making it the largest eruption since the 1991 eruptions of Pinatubo and Hudson. Vertical profiles were retrieved using a line-by-line radiative transfer model and an inversion procedure based on the optimal estimation method (OEM). For the Kasatochi eruption, we found a plume altitude of 12.5 ± 4 km. Taking advantage of IASI's broad spectral coverage, we used the ν_3 band ($\sim$1362 cm^{-1}) and, for the first time, the $\nu_1 + \nu_3$ band ($\sim$2500 cm^{-1}) of SO_2 for the retrievals. While the ν_3 band saturates easily for high SO_2 concentrations, preventing accurate retrieval, the $\nu_1 + \nu_3$ band has a much higher saturation threshold. We also analyzed the broadband signature observed in the radiance spectra in the 1072–1215 cm^{-1} range associated with the presence of aerosols. In the initial volcanic plume the signature matches closely that of mineral ash, while by 10 August most mineral ash is undetectable, and the extinction is shown to match closely the absorption spectrum of liquid H_2SO_4 drops. The extinction by sulphuric acid particles was confirmed by comparing spectra before and a month after the eruption, providing the first spectral detection of such aerosols from nadir view radiance data.

Citation: Karagulian, F., L. Clarisse, C. Clerbaux, A. J. Prata, D. Hurtmans, and P. F. Coheur (2010), Detection of volcanic SO_2, ash, and H_2SO_4 using the Infrared Atmospheric Sounding Interferometer (IASI), *J. Geophys. Res.*, *115*, D00L02, doi:10.1029/2009JD012786.

1. Introduction

[2] Volcanoes can inject gases and particles into the stratosphere. Stratospheric particles have a residence time on the order of 1 year, which contrasts with the short residence time (1 week) for tropospheric particles [*Stephens*, 1990]. A volcanic plume is usually composed of water vapor (H_2O), carbon dioxide (CO_2), sulphur dioxide (SO_2), ash and sulphate aerosols (H_2SO_4). If present in high concentrations, tropospheric sulphur dioxide can damage the environment and human health. In addition, sulphate aerosols can perturb the climate and atmosphere through their radiative forcing [*Robock*, 2000]. Ash and H_2SO_4 emitted by volcanoes can further be a hazard to air traffic [*Casadevall et al.*, 1996]. When ash enters the aircraft's engines, it can melt, as a result of which the engine may fail. In addition, H_2SO_4 is corrosive and can therefore scratch the paint and the windows of the aircrafts, and it can create sulphate deposits in the engine. (http://sacs.aeronomie.be/?kind=pages/aviation). Common tracers of volcanic plumes are ashes and sulfur dioxide (SO_2), which can be tracked up to several days after the eruption. It should be noted though that it is not uncommon for a volcanic plume to split following different trajectories, with a higher SO_2-rich and a lower ash-rich part [*Prata and Kerkmann*, 2007].

[3] Ultraviolet [*Loyola et al.*, 2008] and thermal infrared (TIR) multispectral sounding [*Prata*, 1989a] were mainly used in the past for detection of volcanic SO_2 and volcanic aerosols, respectively. The main types of volcanic aerosols are mineral ash, directly emitted by the eruption and H_2SO_4, which arises from oxidation and hydration of SO_2. Ash can be detected by IR sounding using absorption signatures between 8 and 12 μm (1250 and 833 cm^{-1}), typically centered around 10 μm (1000 cm^{-1}). [*Gangale et al.*, 2010; *Prata*, 1989a, 1989b] and previous works have investigated the detection H_2SO_4 using broadband infrared observations in the atmospheric spectral windows [*Grainger et al.*, 1993]. Data from the Moderate Resolution Imaging Spectrometer (MODIS) instrument was used to develop a global detection algorithm from observations at 8.5, 11 and 12 μm (1176, 909 and 833 cm^{-1}), channels [*Ackerman*, 1997] and characterization of H_2SO_4 in the same channels was made by the High-Resolution Infrared Sounder 2 (HIRS2) on board of the National Oceanic Atmospheric Administration (NOAA) satellites [*Ackerman and Strabala*, 1994]. Extinction coefficients for aerosols of

[1]Spectroscopie de l'Atmosphère, Service de Chimie Quantique Photophysique, Université Libre de Bruxelles, Brussels, Belgium.
[2]UPMC Université Paris 06, Université Versailles St-Quentin, INSU, LATMOS-IPSL, CNRS, Paris, France.
[3]Norwegian Institute for Air Research, Kjeller, Norway.

0148-0227/10/2009JD012786$09.00

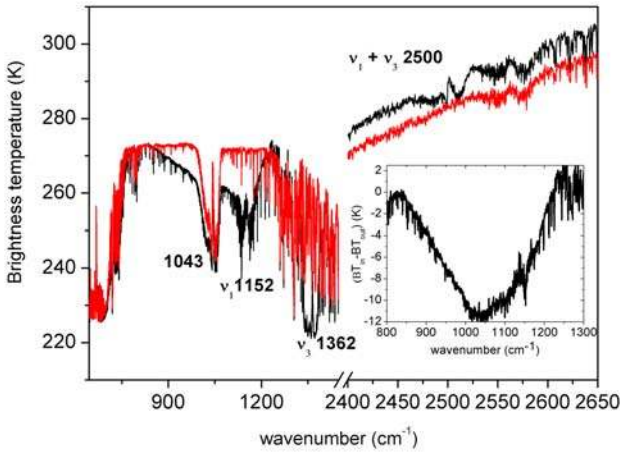

Figure 1. Typical IASI spectra from level 1c (in brightness temperature (BT)) recorded on 8 August 2008 (0914 LT) The spectrum in black was obtained inside the plume of the Kasatochi eruption. The spectrum in red is taken from a nearby pixel, outside the plume. The spectrum in black contains gaseous spectral signatures (H_2O, O_3, N_2O, CH_4, CO_2, and SO_2). Inset shows ratio of the two spectra after removal of gaseous spectral signatures and shows the ash signature.

H_2SO_4 in the upper troposphere were also successfully retrieved from high spectral resolution data recorded by the Michelson Interferometer for Passive Atmospheric Sounding, balloon version (MIPAS-B) in a limb-viewing geometry. Spectral ranges for the MIPAS-B retrieval were: 750–1176 cm^{-1} and 1180–1380 cm^{-1} [*Echle et al.*, 1998; *Prata and Bernardo*, 2007]. Up to now, high spectral resolution IR nadir sounders have not been exploited for detecting H_2SO_4 aerosols, although their usefulness for measuring SO_2 is widely recognized [*Clarisse et al.*, 2008; *Doutriaux-Boucher and Dubuisson*, 2009; *Prata and Bernardo*, 2007]. In this work we investigate detection of SO_2, ash and H_2SO_4 in the infrared by using the Infrared Atmospheric Sounding Interferometer (IASI) observations. For this purpose we investigated the strong 7–8 August 2008 eruption of the Kasatochi volcano, which ejected large quantities of gases and particles directly in the stratosphere. We tracked the plume in space and time and characterized variations of the atmospheric extinction from IASI radiance observations in the atmospheric window. The characterization also included an estimate of the SO_2 emitted mass and plume injection height. Based on the observations, kinetics of SO_2 depletion is provided. A recent work studied the influence on stratospheric aerosols during the first 4 months after the Kasatochi volcano [*Martinsson et al.*, 2009]. That work confirmed that the eruption increased particulate sulfur by a factor up to 10 compared to the period before the eruption. The present paper is structured as follows: section 2 gives a description of the IASI measurements, of the Kasatochi eruption and of the methodology used to retrieve SO_2 profiles from the spectral observation; section 3 presents and discusses the results and section 4 provides the main conclusions. For the retrieval methodology we refer to the recent work by *Clarisse et al.* [2008]. The determination of the radiative properties of aerosols for satellite monitoring or climate studies represents a particular challenge for IASI observations. Therefore, this paper opens perspectives to be a preface for future work that will be performed on the retrieval of different types of aerosols and their radiative properties.

2. Measurements

2.1. IASI Sounding Instrument

[4] IASI is mounted and operated from MetOp-A, a meteorological payload launched by Eumetsat in October 2006 into a polar orbit. This instrument was designed to provide 5 years of global-scale observations of meteorological variables and of a series of key atmospheric gas species with exceptional spatial sampling and coverage. Technical details about IASI and applications for chemistry are explained by *Clerbaux et al.* [2009]. IASI operates in nadir geometry and measures the thermal emission of the Earth/atmosphere. It provides radiance spectra covering the spectral range from 645 to 2760 cm^{-1} without gaps at a spectral resolution of 0.5 cm^{-1} (apodized) and a spectral sampling of 0.25 cm^{-1}. IASI has a field of view sampled by a matrix of 2 × 2 circular pixels of 12 km footprint diameter each at nadir. The measurements are taken along track every 50 km and cross track over 2200 km. In this way, IASI provides global coverage twice daily, once in the morning (around 0930 local time (LT)) and once in the evening (around 2130 LT). It was shown recently that IASI radiances contain important information about traces gases and aerosols [*Clarisse et al.*, 2008; *Clerbaux et al.*, 2009] and a potential to track even short-lived species in space and time, allowing for instance plume chemistry to be studied [*Coheur et al.*, 2009]. Among the numerous trace gas spectral signatures, IASI covers the ν_1, ν_3 and $\nu_1 + \nu_3$ bands of SO_2 as well as volcanic ash and aerosols absorption features between 800 and 1300 cm^{-1}. Its ability to track volcanic plumes and to contribute to operational applications, in particular for aviation hazard has recently been demonstrated by *Clarisse et al.* [2008] (see also http://cpm-ws4.ulb.ac.be/Alerts/).

2.2. August 2008 Kasatochi Eruption

[5] An explosive eruption occurred at Kasatochi volcano (52.18°N, 175.51°W), in Alaska's Aleutian Island Chain, on the afternoon of 7 August 2008. Many volcanoes are located in the Aleutian Island Chain and their activity is irregular. Kasatochi volcano has not been active in the last hundred years, and even reports of eruption in the late 1800s are difficult to confirm. On 8 August 2008, the Alaska volcano Observatory reported that three major explosive eruptions occurred at Kasatochi between approximately 2200 LT on 7 August and 0435 LT on 8 August 2008. The first view of the SO_2 plume emitted by volcano Kasatochi was caught by IASI on 8 August 2008, around 0913 LT. Systematic analysis of IASI spectra recorded in the first hours of the eruption of Kasatochi volcano on 8 August 2008, showed characteristic spectral features for volcanic ash and sulfuric acid aerosols (see Figure 1): in particular the three TIR vibrational bands of SO_2 are observed simultaneously, including the weak $\nu_1 + \nu_3$ combination band. The ash particles were likely removed after a few days, as will be discussed in section 3, while the SO_2 was transported over the entire Northern Hemisphere.

The SO_2 plume was tracked by IASI for over a month (Figure 2).

[6] Different satellite instruments contributed in monitoring the plume on a daily basis. Among these, one of the instrument on board of the NASA's Aura satellite, the ultraviolet Ozone Monitoring Instrument (OMI), identified the dense cloud as containing maximum SO_2 loadings of about 1.5 Tg (http://earthobservatory.nasa.gov/IOTD/view.php?id=8998). The Atmospheric Infrared Sounder (AIRS) on board of the EOS-AURA satellite measured maximum SO_2 loadings of about 1.2 Tg [*Kristiansen*, 2009]. On the other hand, observations from GOME-2 resulted in a estimation of the total SO_2 mass of 2.2 Tg (A. Richter et al., personal communication, 2009). Based on these estimates, the Kasatochi eruption produced obviously one of the largest volcanic SO_2 clouds that scientists have observed since Chile's Hudson volcano erupted in August 1991 ($\sim$3 Tg). However, that is far short of the 20 Tg of SO_2 that Pinatubo injected into the atmosphere in 1991 [*Bluth et al.*, 1993], which had a demonstrated short-term impact on the climate.

[7] Another eruption of the volcano Okmok in the Aleutian Island Chain occurred on 12 July 2008. Measurements from OMI tracked a SO_2 plume moving from the south Aleutians across the North Pacific and then eastward across the United States and Canada. The amount of SO_2 was estimated about 0.1 Tg (http://so2.umbc.edu/omi/pix/special/2008/okmok/okmok_0712.html). Two months earlier, on 2 May 2008, the Chaitén volcano, located in the southern Chile, emitted a small amount of SO_2 of about 5.6×10^{-3} Tg (http://so2.umbc.edu/omi/pix/special/2008/chaiten/chaiten_0502.html). Both these eruptions released also a plume of volcanic ash. The SO_2 plume emitted from Okmok was tracked by IASI during the 14 days following the eruption. According to the Alaska Volcano Observatory (AVO), in early August 2008, Okmok continued releasing a plume of volcanic ash. However, no additional SO_2 emission in the area was observed until the strong explosion Kasatochi on 7 August 2008 sending a cloud of gas and ash high into the atmosphere. The eruptions of Okmok and Kasatochi were hazardous to aviation operations in the area. Both eruptions produced long-lived atmospheric aerosol features detected by the spaceborne Cloud-Aerosol Lidar and Infrared Pathfinder Satellite Observation (CALIPSO). As the SO_2 cloud dispersed, a stratospheric sulfate aerosol layer was observed in the Northern Hemisphere [*Carn et al.*, 2008]. Therefore, from a science perspective, the Kasatochi eruption also provided an opportunity for the observation of stratospheric aerosols. Since the amount of SO_2 emitted from Kasatochi was about 15 times larger than the one from Okmok, the Kasatochi eruption is likely to be the only important source of sulfuric acid aerosols in that time period.

2.3. Trace Gases and Retrieval Approach

[8] As was shown in the recent paper by *Clarisse et al.* [2008], volcanic SO_2 can be adequately tracked from IASI radiance spectra using spectral variations of the brightness temperature (BT) in suitable channels of the ν_3 absorption band. The BT is determined by converting the observed IASI radiance to a blackbody equivalent temperature. The SO_2 plume, from the Kasatochi eruption, was tracked by IASI for a total of 29 days traveling from the Aleutian Islands Chain to Japan at latitudes between 30°N and 90°N [*Rix et al.*, 2008]. Figure 2 shows a sequence of IASI brightness temperature maps illustrating the evolution of the SO_2 plume from 8 August to 6 September 2008. Starting from 11 August the SO_2 plume separated into two parts, one traveling between 30°N and 60°N and the other one between 60°N and 90°N.

[9] For the present spectroscopic analysis, which uses all SO_2 bands and broadband extinction in the atmospheric window, only pixels over the ocean were used in order not to confuse aerosol absorption with surface emissivity features [*DeSouza-Machado et al.*, 2006]. The SO_2 vertical profile and total column measurements were performed using the Atmosphit line-by-line radiative transfer model and retrieval software, developed at the Université Libre de Bruxelles, ULB [*Clerbaux et al.*, 2005; *Coheur et al.*, 2005]. Here only a limited number of retrievals have been performed, small enough not to be computationally demanding, while being representative enough to enable drawing accurate correlations between the observed BT differences and the SO_2 total column. The latter were used to estimate the SO_2 emitted mass. In order to correlate BT differences and SO_2 total columns we used the same method reported in the recent work by *Clarisse et al.* [2008, Figure 9]. For low SO_2 concentrations we found almost linear correlation between BT differences and SO_2 concentration, while for higher concentrations the BT difference progressively saturates.

3. Results

3.1. SO_2 Profiles, Total Emitted Mass, and Depletion Kinetics

[10] Figure 1 (red line) shows a IASI spectrum (in brightness temperature units), recorded inside the volcanic plume during the night of 8 August. It is compared to a spectrum without SO_2 (black line), taken from a nearby pixel outside the plume. High absorption of SO_2 is clearly visible and the following SO_2 bands are seen: the symmetric stretch ν_1 centered at 1152 cm^{-1}, the antisymmetric stretch ν_3 centered at 1362 cm^{-1}, and the weaker $\nu_1 + \nu_3$ combination band at 2500 cm^{-1}. The latter absorption occurs in the range 2400–2650 cm^{-1} where solar reflection can be important [*Herbin et al.*, 2009]. The band at 1043 cm^{-1} is due to ozone. The spectrum also contains spectral features of other stratospheric and tropospheric traces gases, such as H_2O, CO_2, O_3, N_2O, CH_4 and HNO_3. The inset in Figure 1 shows the BT difference ($\Delta BT = BT_{in} - BT_{out}$) between the two spectra, with ozone and SO_2 residual features that were subtracted. In this, the V-shape broadband extinction feature characterizing volcanic aerosols is clearly visible, suggesting significant ash was present in the first few hours after the eruption.

[11] IASI data containing an intrinsic signature for SO_2 were identified by calculating BTs at four different channels. Channels at 1407.25 and 1408.75 cm^{-1} were used to estimate the baseline; 1371.50 and 1371.75 cm^{-1} to estimate absorption in the ν_3 band [*Clarisse et al.*, 2008] and BT differences were calculated by subtracting the baseline from the absorption in the ν_3 band. On 8 August, BT differences up to 36 K were measured using the available signature from the ν_3 band, which corresponds to a SO_2

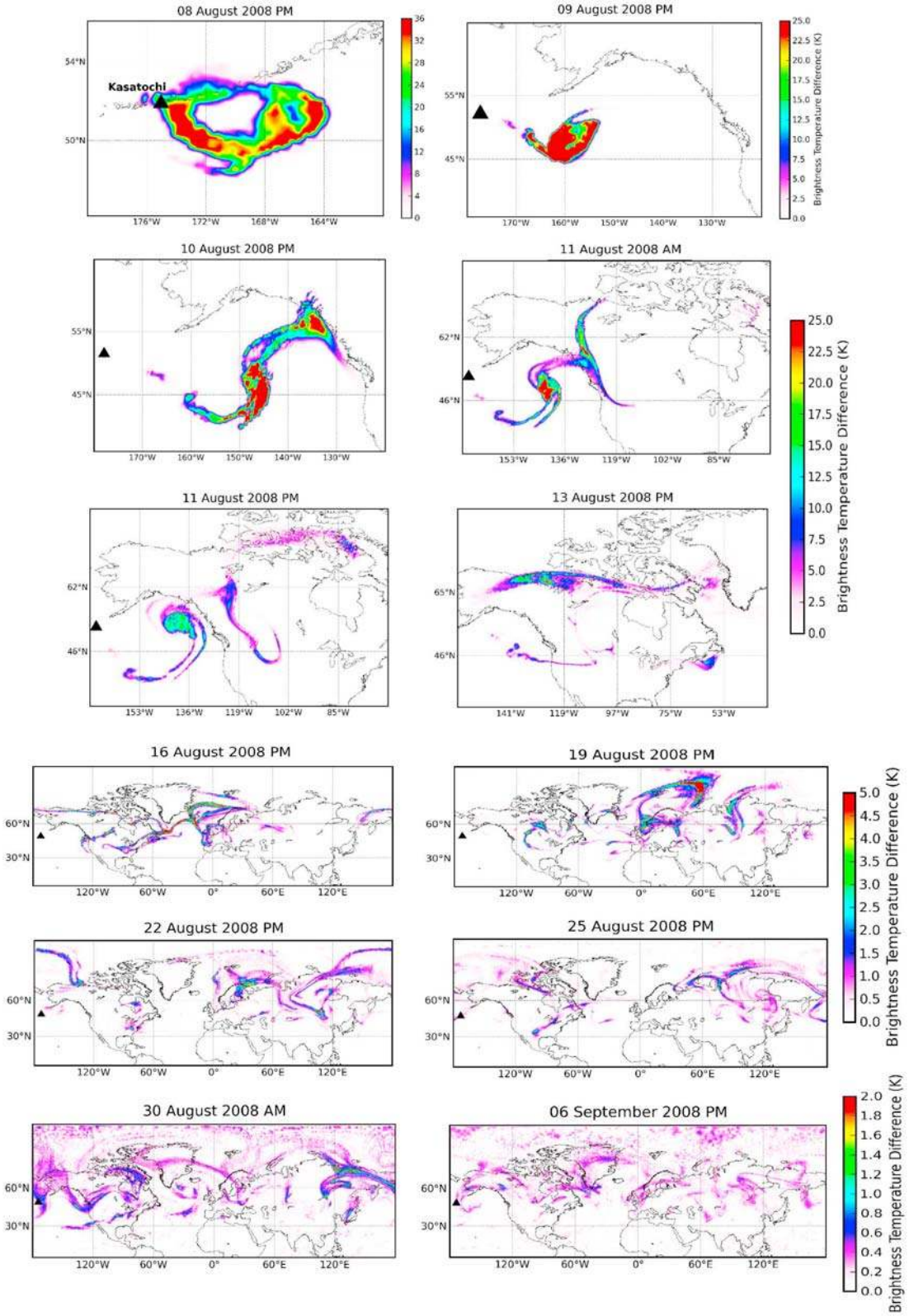

Figure 2. Images of the brightness temperature differences, in Kelvin, for the volcanic plume of SO_2 after the eruption of Kasatochi volcano in August 2008. Time periods AM (before noon) and PM (after noon) are local time.

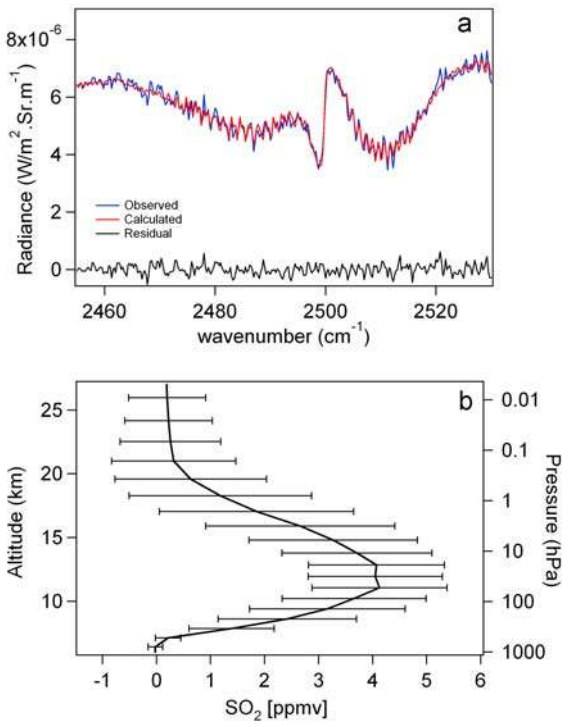

Figure 3. (a) Typical fit of a spectrum recorded on 8 August 2008 (2125 LT) in the spectral range of the $\nu_1 + \nu_3$ combination band for SO_2. The black line corresponds to a RMS of 1.76×10^{-7} W/(m^2 sr m^{-1}). (b) The retrieved vertical profile of SO_2 corresponding to the spectrum shown in Figure 3a.

concentration of 311 DU (1 DU = 2.69×10^{16} molecules cm^{-2}). This estimated concentration of SO_2 was obtained by retrieving the SO_2 profile from 6 km to 21 km in 3 km thick layers using the software Atmosphit and by subsequently matching the resulting column abundance with the brightness temperature, similar to what was done in the recent work by *Clarisse et al.* [2008]. The maximum SO_2 was found at 12.5 ± 4 km, which gives an estimate of the plume's altitude. However, we found that this procedure is not adequate for the first days after the Kasatochi eruption, because of the significant saturation in the ν_3 band due to the large amount of SO_2 emission. Also the ν_1 band could not easily be used to better estimate these quantities (total column and plume's altitude) because of the overlapping extinction features of aerosols. In the work performed by *Clarisse et al.* [2008], the use of the ν_3 band was possible because saturation was not observed even for BT differences as large as 45 K. The reason is that for the Jebel at Tair eruption described in that paper, the SO_2 plume was located around the cold point of the tropopause (16.5 km), allowing larger BT differences without saturation. The Kasatochi plume was richer in SO_2 and located in relative hotter air, explaining why the lower BT differences were accompanied by saturation of the signal.

[12] Therefore, for the first days after the eruption, we used the weaker $\nu_1 + \nu_3$ combination band at ~2500 cm^{-1}. Following a suggestion by *Prata and Bernardo* [2007], we make the first attempt in relying on this band for characterizing the SO_2 content in a volcanic plume. Channels at 2528.5 and 2528.75 cm^{-1} were chosen to estimate the baseline; 2511.25 and 2512.25 cm^{-1} to estimate the BT in the $\nu_1 + \nu_3$ combination band. Solar reflection in the region 2400–2650 cm^{-1} was taken into consideration in the retrieval. Compared with the result obtained from the calculations performed using the ν_3 band, we now measure BT differences up to 17 K on 8 August (for the $\nu_1 + \nu_3$ band) corresponding to a SO_2 concentration of 595 DU, almost twice as large as the previous estimate from ν_3. Full retrieval was carried out in the spectral region 2455–2530 cm^{-1}, considering as interfering molecules CH_4, N_2O and H_2O. Total columns were fitted for the first two, along with water vapor profiles, defined in 2 km thick partial columns from the surface up to 22 km. SO_2 profiles were retrieved as described before, considering five partial columns: 6–9 km, 9–15 km, 15–18 km and 18–21 km. A typical spectral fit and the corresponding vertical profile for one IASI spectrum on nighttime of 8 August are shown in Figures 3a and 3b. The RMS of the fit, 1.76×10^{-7} W/(m^2 sr m^{-1}), is close to the measurement noise of ~1.72×10^{-7} W/(m^2 sr m^{-1}). The peak altitude of the SO_2 plume is found at ~11–13 km with a maximum volume mixing ratio (vmr) of ~4 ppmv (Figure 3b). Considering the limited vertical resolution available from the measurements (averaging kernels, not shown, suggest about 4 km resolution), our best estimate of the plume altitude is 12.5 ± 4 km. This result is in agreement with FLEXPART simulations carried out in a recent study that used OMI data to estimate the SO_2 emission profile of Kasatochi eruption which put the strongest altitude at ~12 km [*Kristiansen*, 2009; *Maerker et al.*, 2008]. Space-based Light Detection and Ranging (LIDAR), such as the Cloud-Aerosols Lidar with Orthogonal Polarization (CALIOP) on board the CALIPSO platform, provide good height estimates for volcanic plume and for aerosol type. Following the Kasatochi eruption, the data from CALIPSO showed the presence of volcanic plume between 5 km and 18 km [*Westphal et al.*, 2008]. These data validate the retrieved height of the volcanic emissions found in the present work.

[13] Spectra recorded after 9 August present values of the BT differences, for the ν_3 band, lower than 30 K and much less aerosol extinction. As a consequence the $\nu_1 + \nu_3$ band becomes at the same time weaker and fully disappears from the spectra on 11 August. Therefore, to estimate the SO_2 amount in the plume after 9 August, we only used the ν_3 band of SO_2, considering more particularly the 1336–1378 cm^{-1} spectral region for the retrievals. In general for low concentrations (<35 DU) we found a linear correlation between the BT differences and SO_2 concentration, while for higher concentrations the BTs difference progressively saturates. From the parameters which best fit the correlation between the BT differences and SO_2 concentration, total columns were evaluated for all IASI spectra in the plume and the emitted mass was calculated by integrating the values over an area containing the plume. After 11 August, the plume split into two branches. The first was transported zonally at about the same latitude as the volcano (52.18°N, 175.51°W), while the second dispersed over the entire Northern Hemisphere northward of ~30°N during the following month.

[14] In summary, BT differences, SO_2 columns and SO_2 total mass in the daily plumes were calculated from $\nu_1 + \nu_3$

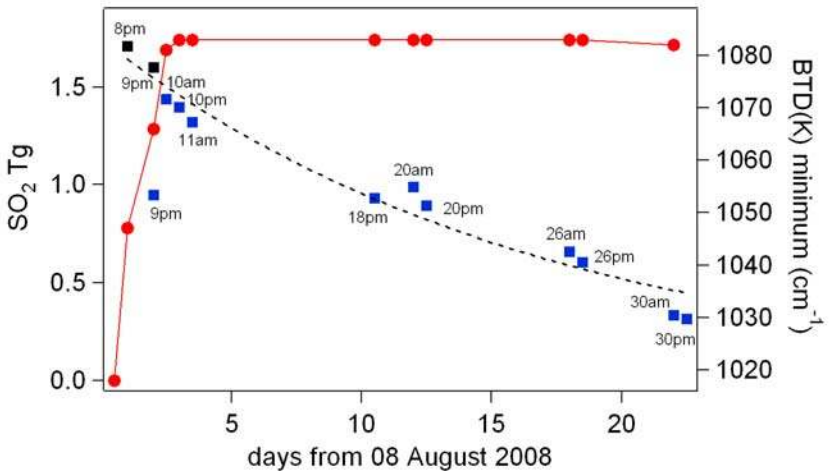

Figure 4. Evolution of the total mass of SO_2 as a function of time (squares). Data for 8 and 9 August 2008 have been obtained from retrievals in the spectral region 2455–2530 cm^{-1} (black squares, $\nu_1 + \nu_3$ combination band). Data from 10 August have been obtained from retrieval in the spectral region 1310–1450 cm^{-1} (blue squares, ν_3 band). Shift of the minimum of absorption for volcanic aerosols in the spectral range 817 and 1215 cm^{-1} (red circles and line) as a function of time. The dotted black line shows the exponential decay of the total mass of SO_2. Time periods am and pm are local time.

for 8 and 9 August and from ν_3 for all subsequent days. The temporal evolution of the total mass of SO_2 is shown in Figure 4 and Table 1. The first day after the eruption, 8 August, it is about 1.7 Tg. The following days, on 9 and 10 August, the amount of SO_2 drastically drops to 1.6 and 1.44 Tg, respectively. This agrees well with estimates from other satellites (see section 2.2).

[15] Interestingly, Figure 4 provides insight into the SO_2 depletion kinetics in the plume. The SO_2 removal rate is relevant to OH chemistry and aerosol formation. Sulfur dioxide is catalytically converted to sulfuric acid by hydroxyl (OH) [*McKeen et al.*, 1984]. The conversion rate is mainly controlled by the reaction $SO_2 + OH \xrightarrow{M} HSO_3$, where M is the total number of air density. As shown in Figure 4, the total mass of SO_2 compares well with the exponential decay $[SO_2] = [SO_2]_0 \exp(-k't)$, where $[SO_2]_0$ is the initial injection of SO_2 and $k' = [M][OH]$ the loss reaction rate. We find a value of $k' \sim 7.0 \times 10^{-7}$ s^{-1} and an e-folding time of 18 days, referred to as time interval in which the initial SO_2 mass has decayed by a factor of e. Previous work on the observed decay of SO_2 from the Pinatubo eruption reported a value of $k' = 5.5 \times 10^{-7}$ s^{-1} [*Read et al.*, 1993], similar to the one found here for the Kasatochi. In that work the loss of SO_2 was consistent with catalytic OH chemical removal in the stratosphere. Also the e-folding time value is in reasonable agreement with the 22 days obtained from FLEXPART simulations for Kasatochi eruption [*Kristiansen*, 2009].

3.2. Aerosol Extinction and Sulfuric Acid Particles

[16] The refractive index of different scattering species leads to specific spectral signatures [*Bohren and Huffman*, 1983], that affects IASI radiances in several ways. For instance, volcanic aerosols such as ash and sulfuric acid absorb less at 833 and 1250 cm^{-1} than at 980 cm^{-1}, yielding the so-called "V"-shape depression of the BT across the thermal IR window (see Figure 1). Similarly to what was done above for SO_2, aerosol identification can be achieved by calculating BT differences in channels sensitive to the broadband extinction features. As already discussed above, inset in Figure 1 shows the BT difference ($\Delta BT = BT_{in} - BT_{out}$) between a spectrum taken from inside and outside the plume on the first day after the eruption. Using this spectral information, we have selected channels at 982 and 1072 cm^{-1} to track the aerosol plume, with channels at 817.75 and 1215.15 cm^{-1} that are used to estimate the baseline. This selection of channels avoids the main interferences, due to the presence of ozone and SO_2. Because the detection of stratospheric and tropospheric aerosols over land is complicated by spectral variation in surface emissivity, only IASI spectra recorder over ocean regions, which have spectrally uniform emissivity [*Stephens*, 1990], were selected. Figure 5 shows the sequence of the BT differences

Table 1. Summary of the Observations and Assignments of the Infrared Bands Used for the Retrievals of SO_2 Total Mass and Aerosols Species From the IASI Spectra During the Days After the Kasatochi Eruption

August 2008[a]	SO_2 Band (cm^{-1})	SO_2 Total Mass (Tg)	Aerosols (1072–1215 cm^{-1})
8 pm	$\nu_1 + \nu_3$ (~2500)	1.71	ash
9 pm	$\nu_1 + \nu_3$	1.60	ash + H_2SO_4
10 am	ν_3 (~1362)	1.44	ash + H_2SO_4
10 pm	ν_3	1.398	H_2SO_4
11 am	ν_3	1.320	H_2SO_4
18 pm	ν_3	0.932	H_2SO_4
20 am	ν_3	0.990	H_2SO_4
20 pm	ν_3	0.892	H_2SO_4
26 am	ν_3	0.660	H_2SO_4
26 pm	ν_3	0.606	H_2SO_4
30 am	ν_3	0.334	H_2SO_4
30 pm	ν_3	0.315	H_2SO_4

[a]Given are date in August and time of day (am and pm are before noon and after noon, respectively, in local time).

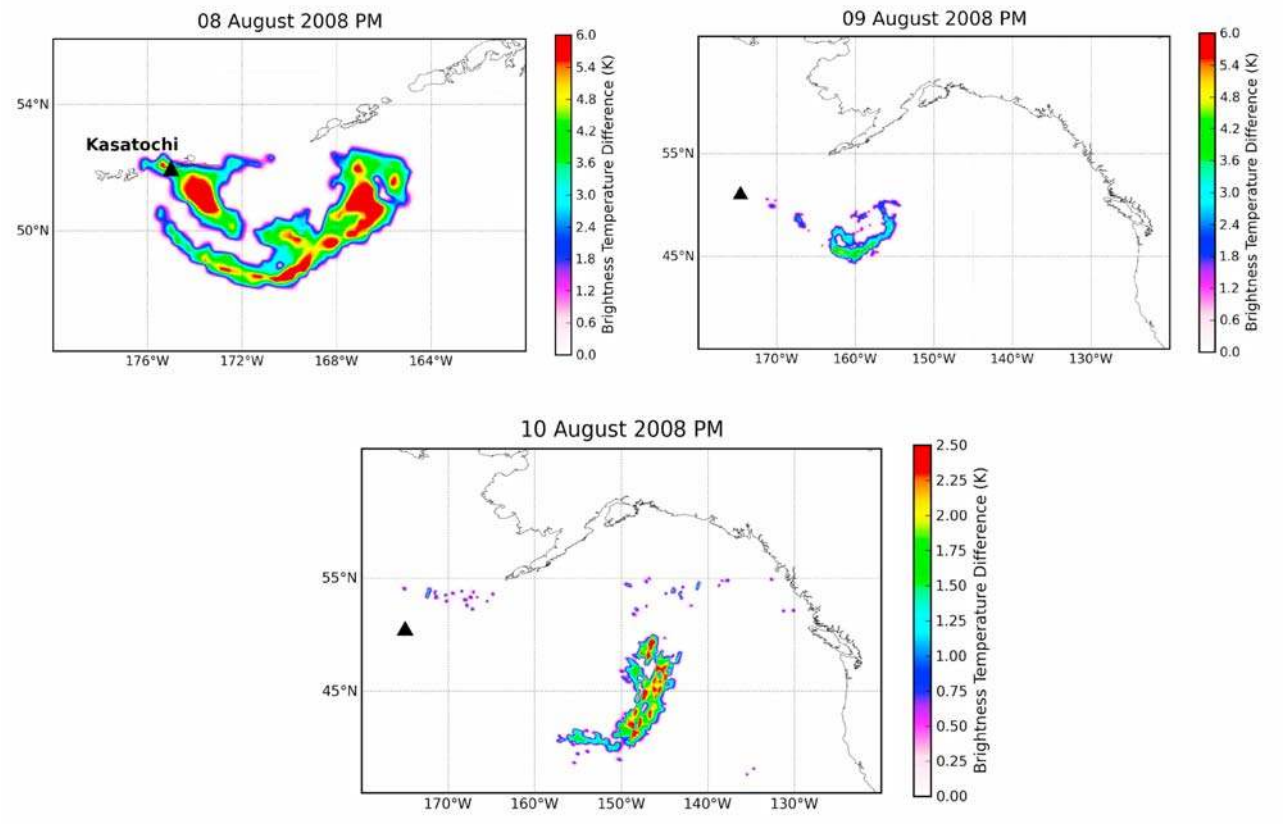

Figure 5. Different views of the volcanic aerosols plume from the eruption of the Kasatochi volcano in August 2008. Brightness temperature differences between IASI channels at 1072 and 1215 cm^{-1} were used to follow the aerosol plume. Time periods AM and PM are in local time.

(BT_{1072} - BT_{1215}) during the first 3 days that followed the eruption. We can observe that the location of the aerosol plume coincides with the location of the SO_2 plume. Considering also that volcanic ash is usually removed within a few days, this may be an indication that the particulate phase in the plume consists of both ash and SO_2 oxidation products, such as H_2SO_4.

[17] In order to confirm this, and relying on the specific extinction properties of volcanic ash and sulfuric acid particles, we analyzed the BT spectra, with the aim to differentiate the two particle types. Figure 6 shows smoothed spectra of the BT difference spectra during the first 3 days 8, 9 and 10 August after the Kasatochi eruption. All curves in Figure 6 show the "V′" shape characteristic of volcanic aerosols absorption in the region 800–1215 cm^{-1}. However, the spectral details of this broadband extinction vary, possibly indicating modification of the physical and chemical properties of the aerosol. Figure 6 (black line) shows a representative spectrum for the morning of 8 August with the minimum of absorbance centered at 1018 cm^{-1}. Starting from the afternoon of 8 August, the minimum progressively shows a "blue" shift of several wave numbers with time and in the afternoon of 8 August the minimum is at 1047 cm^{-1}. In the following days of 9 and 10 August, the minimum is at 1066 and 1081 cm^{-1}, respectively. The shift of this minimum is accompanied by a dramatic decrease of the slope of BT_{1072} - BT_{1215}. In order to explain this, we have performed a series of radiative transfer simulations for aerosols using a Mie type code [*Mie*, 1908], assuming a plane-parallel atmosphere. We tried several particle types and sizes and compared the simulations with the observations. The properties influencing the spectral shape and the magnitude of the aerosol extinction are size distribution, geometrical shape and composition of the aerosols particles. Stratospheric sulfuric acid is composed of liquid droplets than can be assumed to be spherical [*Tolbert*, 1994]. The chemical composition of the aerosol particles determines the complex refractive index of which the imaginary part is equivalent to the absorption cross section. The complex refractive index is a function of wave number revealing broadband minima due to absorption bands of the different ions present in the aerosols particle. Thus the spectral shape of the aerosols extinction is predominantly characterized by the particle composition. Figure 7 shows simulated BT of an atmosphere with a single layer of volcanic ash of radius r = 0.75 μm at a density n of 8.0 $\times$ 10^7 particles/cm^2. The overlap between the computed Mie curve and the observed BT difference spectrum in Figure 7 is excellent and shows that the ash present in the volcanic plume during the daytime of 8 August strongly dominates the particulate phase. Starting from 8 August, the ash-only extinction is no longer sufficient to reproduce the observation, especially above 1100 cm^{-1} where H_2SO_4 aerosols are likely to contribute. Previous work showed that the composition of sulphuric acid–water droplets depends on the atmospheric temperature and water vapor partial pressure [*Steele and*

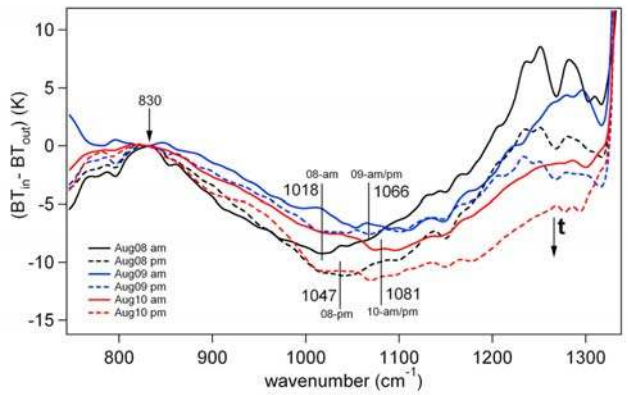

Figure 6. Smoothed brightness temperature differences spectra ($\Delta B = BT_{in} - BT_{out}$) between two spectra taken from inside and outside the SO_2 plume during the days 8, 9, and 10 August 2008. A Gaussian filter has been used for the binomial smoothing operation. The spectra show a clear "V" shape depression between ~833 and ~1250 cm^{-1} characteristic for the additional continuum due to the presence of volcanic aerosols. Time periods am and pm are in local time.

Hamill, 1981; *Tolbert*, 1994]. In the present work the simulation has been carried out with a solution of 75% H_2SO_4 and 25% H_2O with droplets of radius $r = 1.2$ μm at a density n of 5.0×10^6 particles/cm^2. For the simulation with aerosols of H_2SO_4 we used the indices of refraction reported by *Rublev* [1994]. As can be seen in Figure 7, the computed Mie curve for H_2SO_4-H_2O aerosols best overlap the BT difference spectrum corresponding to the volcanic plume for the nighttime of 10 August. This notably reproduces the change of extinction shape at wave numbers higher than 1000 cm^{-1} as compared to the 8 August situation. In the simulated BT spectrum of H_2SO_4 aerosols we find three local minima (approximately at 904, 1042 and 1160 cm^{-1}), which correspond with the local minima of the imaginary part of the complex refraction index for a 75% H_2SO_4-H_2O solution [*Grainger et al.*, 1993]. Interestingly, previous work showed that variation in droplets radius only affects the wavelengths in the range 1160–1215 cm^{-1} [*Grainger et al.*, 1993]. Outside this range the extinction is weakly dependent on the drop size and on the refraction index (Figure 6). This is because the scattering properties of these aerosols are close to the Rayleigh approximation (the size parameter $2\pi r \leq \lambda$). In the case of particle radii being small in comparison with the wavelength, the extinction coefficient is sensitive to the total particle volume but not to the shape of the particle size distribution. This is the Rayleigh limit of the Mie Theory [*Bohren and Huffman*, 1983]. In this case, the size of the aerosols simply scales the absorption for all wavelengths similarly. This conclusion is also consistent with the investigation carried out by *Halperin and Murcray* [1987], who calculated the absorption coefficients of El Chichón aerosol size distributions. However, the observed change in the slope of BT_{1072} - BT_{1215} shown in Figure 6 is due to the fact that the Rayleigh approximation is not quite true for very strong absorption of H_2SO_4 aerosols at 1176–1250 cm^{-1} (8–8.5 μm). This might also be correlated to the fact that the imaginary part of the refractive index reaches a minimum at 8.5 μm (1176 cm^{-1}) which corresponds to the region of maximum absorption by the H_2SO_4 aerosols [*Grainger et al.*, 1993].

[18] The absorption optical density is proportional to $nV_p\lambda$, where n is the number of density, V_p the volume of the droplets and λ the wavelength. Therefore, as seen from the present results, for a fixed nV_p the effect of the aerosols is very similar as long as the particle size r is less than ~2 μm. The imperfect match between observations and the H_2SO_4-H_2O simulations between 8 August in the afternoon and 10 August in the morning thus suggests that, starting a few hours to a day after the eruption, ash and growing H_2SO_4 aerosols coexist in the volcanic plume, after which ash is removed and only the sulfuric acid particles remain. This latter conclusion is confirmed by the fact that later in August the minimum of the BT difference spectra (see Figure 6 for 18, 25 and 30 August) remains located at ~1081 cm^{-1}. In addition, the slope of BT_{1072} - BT_{1215} remains constant but the amplitude of the extinction decreases, suggesting a progressive dilution of the sulfuric acid particles in ambient air.

[19] In order to assess whether H_2SO_4 was still present after 1 month from the Kasatochi eruption, we have averaged BT spectra of 5 August and 1 month later at 6 September in the Northern Hemisphere and compared them together. For 6 September, we took only spectra with BT differences in the ν_3 band higher than 0.5 K, because even after a month, the plume did not spread homogeneously over the Northern Hemisphere. Figure 8 shows the BT difference between the averaged spectra of 5 August and 6 September. As can be seen, the spectrum shows the "V′" shape characteristic of aerosols in the region 750–1300 cm^{-1} but with clear local minima at approximately 904, 1042 and 1160 cm^{-1}, matching the expected H_2SO_4 aerosols extinction. This is the strongest evidence of H_2SO_4 we found in IASI spectra. Note that the baseline of the spectra

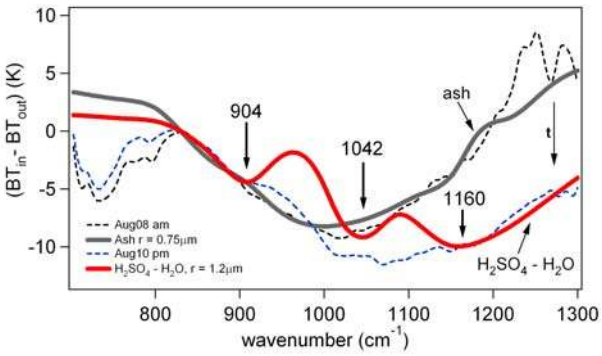

Figure 7. Smoothed brightness temperature differences spectra ($\Delta B = BT_{in} - BT_{out}$) between two spectra taken from inside and outside the SO_2 plume during daytime of 8 August and nighttime of 10 August 2008 (dashed lines). Simulated brightness temperatures of an atmosphere with a single layer of volcanic ash ($r = 0.75$ μm, $n = 8.0 \times 10^7$ particles/cm^2, gray line). Simulation of brightness temperature of an atmosphere with a single layer of a solution of 75% H_2SO_4 and 25% H_2O water droplets ($r = 1.2$ μm, $n = 5.0 \times 10^6$ particles/cm^2, red line). Simulations have been carried out using Mie theory.

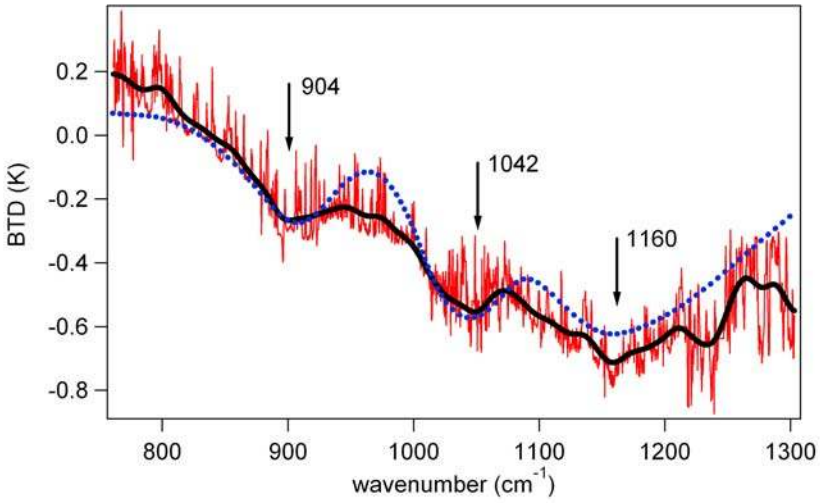

Figure 8. Brightness temperature difference spectrum between averaged spectra recorded 2 days before (5 August 2008) and 1 month after the Kasatochi eruption (6 September 2008). Spectra have been averaged over the Northern Hemisphere. Red and black lines represent the raw and smoothed brightness temperature difference spectrum, respectively. Dashed blue line represents the simulated brightness temperature of an atmosphere with a single layer of a solution of 75% H_2SO_4 and 25% H_2O water droplets (r = 1.2 μm, n = 5.0 $\times$ 10^6 particles/cm^2).

in Figure 8 has been shifted by 4 K from its initial value which corresponds to the average temperature variation between the two time periods.

4. Conclusions

[20] This study provides a detailed characterization of the Kasatochi August 2008 plume and of its spatial and temporal evolution, using IASI high spectral resolution infrared radiance measurements, using on one hand signatures of SO_2 and on the other hand, broadband extinction features of aerosols. We have estimated a total ejected mass of SO_2 by the Kasatochi eruption to be 1.7 Tg, using absorption of SO_2 in the ν_3 band but also, for the first time, in the much weaker $\nu_1 + \nu_3$ combination band during the first day, when the signal of ν_3 strongly saturates. The plume mean altitude was estimated at 12.5 $\pm$ 4 km from SO_2 profile retrievals. We have followed the plume transport for more than a month and investigated the SO_2 loss rate: a kinetic constant $k' \sim 7.0 \times 10^{-7}$ s^{-1} was calculated, corresponding to an e-folding time of 18 days. All values were found to be in good agreement with existing literature. SO_2 oxidation likely results in the formation of H_2SO_4-H_2O aerosols, which were confidently identified in the spectra using broadband signatures in the atmospheric window. We have found convincing evidence that a few hours after the eruption only ash particles were present in the plume, progressively replaced by a mixture with sulfuric acid particles. After a few days, only the latter type remained. Sulfuric acid particles were still observed, although highly diluted, more than a month after the eruption. By the simultaneous observation of volcanic SO_2 and aerosols, and possibly the tracking of the aerosol plume, high spectral resolution infrared remote-sensing measurements offer great potential for the operational surveillance of volcanic activity and for studying the impact of large eruption on chemistry and climate.

[21] **Acknowledgments.** IASI has been developed and built under the responsibility of the Centre National d'Etudes Spatiales (CNES, France). It is flown onboard the Metop satellites as part of the EUMETSAT Polar System. The IASI L1 data are received through the EUMETCast near real time data distribution service. The research in Belgium was funded by the F.R.S.-FNRS (M.I.S. nF.4511.08), the Belgian State Federal Office for Scientific, Technical and Cultural Affairs and the European Space Agency (ESA-Prodex arrangements C90–327). L. Clarisse and P. F. Coheur are Research Associates and Scientific Research Workers with the FRS-F.N.R.S, Belgium. Financial support by the " Communauté française de Belgique—Actions de Recherche Concertées " is also acknowledged. The authors wish to thank Antoine Depauw for his assistance. C. Clerbaux is grateful for the CNES financial support. A. J. Prata acknowledges the support of the European Space Agency under the Support to Aviation for Volcanic Ash avoidance (SAVAA) project.

References

Ackerman, S. A. (1997), Remote sensing aerosols using satellite infrared observations, *J. Geophys. Res.*, *102*(D14), 17,069–17,079, doi:10.1029/96JD03066.

Ackerman, S. A., and K. I. Strabala (1994), Satellite remote-sensing of H_2SO_4 aerosol using the 8 to 12 μm window region: Application to Mount Pinatubo, *J. Geophys. Res.*, *99*(D9), 18,639–18,649, doi:10.1029/94JD01331.

Bluth, G. J. S., C. C. Schnetzler, A. J. Krueger, and L. S. Walter (1993), The contribution of explosive volcanism to global atmospheric sulfur-dioxide concentrations, *Nature*, *366*(6453), 327–329, doi:10.1038/366327a0.

Bohren, C. F., and D. F. Huffman (1983), *Absorption and Scattering of Light by Small Particles*, John Wiley, Hoboken, N. J.

Carn, S. A., N. A. Krotkov, V. Fioletov, K. Yang, A. J. Krueger, and D. Tarasick (2008), Emission, transport and validation of sulfuric dioxide in the 2008 Okmok and Kasatochi eruption clouds, *Eos Trans. AGU*, *89*(53), Fall Meet. Suppl., Abstract A51J-07.

Casadevall, T. J., P. J. Delos Reyes, and D. J. Schneider (1996), The 1991 Pinatubo eruptions and their effects on aircraft operations, in *Fire and Mud: Eruptions and Lahars of Mount Pinatubo, Philippines), Quezon City: Philippines Institute of Volcanology and Seismology*, edited by C. G. Newhall and R. S. Punongbayan, pp. 625–636, Univ. of Wash. Press, Seattle.

Clarisse, L., P. F. Coheur, A. J. Prata, D. Hurtmans, A. Razavi, T. Phulpin, J. Hadji-Lazaro, and C. Clerbaux (2008), Tracking and quantifying

volcanic SO_2 with IASI, the September 2007 eruption at Jebel at Tair, *Atmos. Chem. Phys.*, *8*(24), 7723–7734.

Clerbaux, C., P. F. Coheur, D. Hurtmans, B. Barret, M. Carleer, R. Colin, K. Semeniuk, J. C. McConnell, C. Boone, and P. Bernath (2005), Carbon monoxide distribution from the ACE-FTS solar occultation measurements, *Geophys. Res. Lett.*, *32*, L16S01, doi:10.1029/2005GL022394.

Clerbaux, C., et al. (2009), Monitoring of atmospheric composition using the thermal infrared IASI/MetOp sounder, *Atmos. Chem. Phys.*, *9*, 6041–6054.

Coheur, P. F., B. Barret, S. Turquety, D. Hurtmans, J. Hadji-Lazaro, and C. Clerbaux (2005), Retrieval and characterization of ozone vertical profiles from a thermal infrared nadir sounder, *J. Geophys. Res.*, *110*, D24303, doi:10.1029/2005JD005845.

Coheur, P. F., L. Clarisse, S. Turquety, D. Hurtmans, and C. Clerbaux (2009), IASI measurements of reactive trace species in biomass burning plumes, *Atmos. Chem. Phys.*, *9*, 5655–5667.

DeSouza-Machado, S. G., L. L. Strow, S. E. Hannon, and H. E. Motteler (2006), Infrared dust spectral signatures from AIRS, *Geophys. Res. Lett.*, *33*, L03801, doi:10.1029/2005GL024364.

Doutriaux-Boucher, M., and P. Dubuisson (2009), Detection of volcanic SO_2 by spaceborne infrared radiometers, *Atmos. Res.*, *92*(1), 69–79, doi:10.1016/j.atmosres.2008.08.009.

Echle, G., T. von Clarmann, and H. Oelhaf (1998), Optical and microphysical parameters of the Mt. Pinatubo aerosol as determined from MIPAS-B mid-IR limb emission spectra, *J. Geophys. Res.*, *103*(D15), 19,193–19,211, doi:10.1029/98JD01363.

Gangale, G., A. Prata, and L. Clarisse (2010), On the infrared spectral signature of volcanic ash, *Remote Sens. Environ.*, *114*(2), 414–425.

Grainger, R. G., A. Lambert, F. W. Taylor, J. J. Remedios, C. D. Rodgers, M. Corney, and B. J. Kerridge (1993), Infrared absorption by volcanic stratospheric aerosols observed by ISAMS, *Geophys. Res. Lett.*, *20*(12), 1283–1286, doi:10.1029/93GL00823.

Halperin, B., and D. G. Murcray (1987), Effect of volcanic aerosols on stratospheric radiance at wavelengths between 8 and 13 μm, *Appl. Opt.*, *26*(11), 2222–2235, doi:10.1364/AO.26.002222.

Herbin, H., D. Hurtmans, C. Clerbaux, L. Clarisse, and P. F. Coheur (2009), $H_2^{16}O$ and HDO measurements with IASI/MetOp, *Atmos. Chem. Phys.*, *9*, 9433–9447.

Kristiansen, N. I. (2009), Determination of the emission height profile of volcanic emissions using inverse modelling, Master's thesis, 82 pp., Dep. of Geosci., Univ. of Oslo, Oslo, Norway.

Loyola, D., J. van Geffen, P. Valks, T. Erbertseder, M. V. Roozendael, W. Thomas, W. Zimmer, and K. Wibkirchen (2008), Satellite based detection of volcanic sulphur dioxide from recent eruptions in Central and South America, *Adv. Geosci.*, *14*, 35–40.

Maerker, K. C., P. V. M. Rix, and J. van Geffen (2008), Trajectory matching and dispersion modeling of volcanic plumes utilizing space-observations, paper presented at 2nd USEReST Workshop, Inst. of Electr. and Electron. Eng., Naples, Italy.

Martinsson, B. G., C. A. M. Brenninkmeijer, S. A. Carn, M. Hermann, K.-P. Heue, P. F. J. van Velthoven, and A. Zahn (2009), Influence of the 2008 Kasatochi volcanic eruption on sulfurous and carbonaceous aerosols constituents in the lower stratosphere, *Geophys. Res. Lett.*, *36*, L12813, doi:10.1029/2009GL038735.

McKeen, S. A., S. C. Liu, and C. S. Kiang (1984), On the chemistry of stratospheric SO_2 from volcanic eruptions, *J. Geophys. Res.*, *89*(D3), 4873–4881, doi:10.1029/JD089iD03p04873.

Mie, G. (1908), Beigrade zur Optik trüber Medin, speziell kolloidaler Metallösungen, *Ann. Phys.*, *25*, 377–455, doi:10.1002/andp.19083300302.

Prata, A. J. (1989a), Observations of volcanic ash clouds in the 10–12 μm window using AVHRR/2 data, *Int. J. Remote Sens.*, *10*(4–5), 751–761, doi:10.1080/01431168908903916.

Prata, A. J. (1989b), Infrared radiative transfer calculations for volcanic ash clouds, *Geophys. Res. Lett.*, *16*(11), 1293–1296, doi:10.1029/GL016i011p01293.

Prata, A. J., and C. Bernardo (2007), Retrieval of volcanic SO_2 column abundance from atmospheric infrared sounder data, *J. Geophys. Res.*, *112*, D20204, doi:10.1029/2006JD007955.

Prata, A. J., and J. Kerkmann (2007), Simultaneous retrieval of volcanic ash and SO_2 using MSG-SEVIRI measurements, *Geophys. Res. Lett.*, *34*, L05813, doi:10.1029/2006GL028691.

Read, W. G., L. Froidevaux, and J. W. Waters (1993), Microwave Limb Sounder measurement of stratospheric SO_2 from the Mt. Pinatubo Volcano, *Geophys. Res. Lett.*, *20*(12), 1299–1302, doi:10.1029/93GL00831.

Rix, M., P. Valks, N. Hao, T. Erbertseder, and J. van Geffen (2008), Monitoring of volcanic SO_2 emissions using GOME-2 satellite instrument, paper presented at 2nd USEReST Workshop, Inst. of Electr. and Electron. Eng., Naples, Italy.

Robock, A. (2000), Volcanic eruptions and climate, *Rev. Geophys.*, *38*, 191–219, doi:10.1029/1998RG000054.

Rublev, A. A. (1994), Algorithm and computation of aerosol phase functions, *Internal Note IAE-5715/16*, Kurchatov Inst., Moscow.

Steele, H. M., and P. Hamill (1981), Effects of temperature and humidity on the growth and optical properties of sulphuric acid-water droplets in the stratosphere, *J. Aerosol Sci.*, *12*, 517–529, doi:10.1016/0021-8502(81)90054-9.

Stephens, G. L. (1990), On the relationship between water-vapor over the oceans and sea-surface temperature, *J. Clim.*, *3*(6), 634–645, doi:10.1175/1520-0442(1990)003<0634:OTRBWV>2.0.CO;2.

Tolbert, M. A. (1994), Sulfate aerosols and polar stratospheric cloud formation, *Science*, *264*(5158), 527–528, doi:10.1126/science.264.5158.527.

Westphal, D. L., H. Chen, J. R. Campbell, K. Richardson, J. D. Doyle, and M. D. Fromm (2008), Numerical investigation and forecasting of the Kasatochi ash plume, *Eos Trans. AGU*, *89*(53), Fall Meet. Suppl., Abstract A53B-0267.

L. Clarisse, P. F. Coheur, D. Hurtmans, and F. Karagulian, Spectroscopie de l'Atmosphère, Service de Chimie Quantique Photophysique, Université Libre de Bruxelles, Brussels B-1050, Belgium. (fkaragul@ulb.ac.be)

C. Clerbaux, UPMC Université Paris 06, Université Versailles St-Quentin, INSU, LATMOS-IPSL, CNRS, F-75252 Paris CEDEX 05, France.

A. J. Prata, Norwegian Institute for Air Research, N-2027 Kjeller, Norway.